

Electric Field Alignment of Symmetric Diblock Copolymer Thin Films

Ting Xu, Yuqing Zhu,[†] Samuel P. Gido, and Thomas P. Russell*

Department of Polymer Science and Engineering, University of Massachusetts, Amherst, Massachusetts 01003

Received December 1, 2003; Revised Manuscript Received January 20, 2004

ABSTRACT: The alignment of thin films of symmetric diblock copolymer of polystyrene and poly(methyl methacrylate), PS-*b*-PMMA, in an electric field was studied as a function of film thickness and interfacial energy using small-angle neutron scattering and transmission electron microscopy. There is a competition between the applied electric field, aligning the microdomains normal to the surface, and surface fields that tend to align the microdomains parallel to the surface. For films with thickness $t < 10L_0$, where L_0 is the equilibrium period of the copolymer in the bulk, interfacial interactions are dominant, and the lamellar microdomains orient parallel to the substrate surface regardless of the applied electric field. If $t > 10L_0$, interfacial interactions become less important, and lamellar microdomains in the center of the films could be oriented in the direction of the applied field, i.e., normal to the surface. Transmission electron microscopy shows that the dominant mechanism of orientation is one where the lamellae are locally disrupted and re-form with an orientation in the direction of the applied field.

Introduction

Block copolymers self-assemble into arrays of microdomains, e.g. lamellae, cylinders, or spheres depending on the volume fraction of the components and χN , where χ is the Flory–Huggins segmental interaction parameter and N is the degree of polymerization. The sizes of the microdomains are predominantly dictated by the total molecular weight of the copolymer and, hence, are tens of nanometers in size.¹ Locally, the ordering of the domains is high, but globally the arrays of grains form where the orientation of the grains, on average, is random. External fields, such as shear,^{2–4} electric,^{5,6} and surface fields,⁷ have been used in both the bulk and thin films to affect alignment.^{2–11} The preferential interaction and consequent segregation of one block to the substrate orients the microdomains parallel to the substrate surface.^{11–13} Electric fields normal to the surface have been used to overcome interfacial interactions and orient the microdomains in the direction of the applied field.⁵ Neglecting confinement effects, the critical electric field strength needed to orient the microdomains is given by^{14,15}

$$E_c = \Delta\gamma^{1/2} \frac{2(\epsilon_A + \epsilon_B)^{1/2}}{\epsilon_A - \epsilon_B} t^{-1/2} \quad (1)$$

where $\Delta\gamma$ is the difference between the interfacial energies of each block with the substrate, ϵ_A and ϵ_B are the static dielectric constants of block A and B, respectively, and t is the film thickness. Thus, from eq 1, it is seen that either the film thickness or $\Delta\gamma$ can prevent or limit the orientation of the copolymer microdomains. If $\Delta\gamma$ is too large or the film is too thin, E_c is greater than the dielectric breakdown, and microdomain orientation is not possible. If $\Delta\gamma = 0$, i.e., when interfacial interactions are balanced, then $E_c = 0$.

The orientation of diblock copolymers has been studied in both the bulk and solution.^{8–10,16,17} Theoretically, Onuki and Fukuda investigated the dynamics of undu-

lations in two-dimensional lamellar systems as a route toward alignment.¹⁸ Amundson et al. studied the interactions of defects and defect mobility as a means of microdomain reorientation. Using TEM, they showed evidence of defect movement and subsequent annihilation of defect structures in bulk copolymer samples.^{8–10} Recently, Krausch and co-workers studied the electric field alignment of concentrated copolymer solutions by the real-time synchrotron SAXS measurements and have shown that close to the order–disorder transition (ODT) migration of grain boundaries is the dominant mechanism, while rotation of grains dominates further away from the ODT, i.e., under strongly segregating conditions.^{16,17} They argued that the viscosity plays a key role in determining the mechanism of the orientation. Zvelindovsky et al. simulated the same alignment process and showed that the mechanism by which the orientation occurs is determined by the magnitude of the interactions between the two blocks, which is related to the segmental interaction parameter χ_{AB} .¹⁹ In the strong segregation limit where χ_{AB} is large, it costs more energy to deform the microdomains due to the increase in interfacial area resulting from these deformations. They also studied dynamics of mesophase formation in the framework of dynamic density functional theory (DFT) for a diblock copolymer melt. Under an electric field, the domain alignment is achieved by a relatively local defect movement, i.e., the lamellae locally break up and merge again.²⁰ De Rouchey et al. have also recently argued, from small-angle X-ray scattering results, that the copolymer domains in thick films are initially disrupted to create smaller grains that can rotate more easily in the field.²¹ The presence of two interfaces in thin films amplifies the importance of interfacial interactions that become increasingly more dominant as the film gets thinner. In addition, with decreasing thickness, confinement of the morphology in the thickness direction can present a geometric barrier. Grain rotation, for example, may not be possible due to this film thickness constraint.

In the present study the dependence of the electric field alignment of a symmetric diblock copolymer polystyrene-*b*-poly(methyl methacrylate), PS-*b*-PMMA, was

[†] Current address: Eastman Chemical, Kingsport, TN.

* To whom correspondence should be addressed.

studied as a function of film thickness using in-situ small-angle neutron scattering (SANS) and transmission electron microscopy (TEM). It is shown that the orientation in thin films is a competition between the applied electric field that aligns the microdomains normal to the surface and the surface fields that align the microdomains parallel to the surface. For very thin films, surface-induced orientation dominates, and the lamellar microdomains are always parallel to the substrate surface. With increasing film thickness, surface effects diminish with distance, and the applied field orients the lamellar microdomains in the center of the film in the direction of the applied field. The intermediate and late stages of the alignment were studied using transmission electron microscopy. Results from these studies indicate that the lamellae locally break up and then re-form, in agreement with the arguments of DeRouchey et al. and Zvelindovsky et al.^{19–21}

Experimental Section

Symmetric diblock copolymers of polystyrene and poly(methyl methacrylate), PS-*b*-PMMA, with a number-average molecular weight of 7.19×10^4 g/mol and a PS volume fraction of 0.5 with a polydispersity of 1.09 were synthesized anionically. SANS studies were performed with PS-*b*-PMMA where the polystyrene block was deuterated, denoted as dPS-*b*-PMMA. The molecular weight of dPS-*b*-PMMA was 7.05×10^4 g/mol with a polydispersity of 1.05 and a dPS volume fraction of 0.5. Both copolymers have order-disorder transition temperatures (ODT) higher than 250 °C and could not be determined due to the sample degradation. Films were prepared by spin-coating a toluene solution of the copolymer onto a substrate. Film thickness was controlled by varying the solution concentration and spinning speed. An aluminized Kapton film was used as a top electrode, where a thin (20–25 μm) layer of cross-linked poly(dimethylsiloxane) (PDMS) (Sylgard) was used as buffer layer between the Kapton electrode and the copolymer thin film. The interfacial energy of PS with PDMS is lower than that of PMMA with PDMS as indicated by X-ray photoelectron spectroscopy. The preparation of the cross-linked PDMS layer has been described previously.²² Using this setup, ~ 40 V/ μm is the highest electric field strength experimentally feasible.

Transmission small-angle neutron scattering (SANS) experiments were performed on beamline NG-3, a 30 m SANS instrument at National Institute of Standard Technology (NIST), using neutrons with a wavelength $\lambda = 0.6$ nm and $\Delta\lambda/\lambda = 15\%$. For the in-situ SANS studies, the spin-coated samples were dried at 25 °C under vacuum to remove solvent. In the SANS experiment, the samples were heated from room temperature to 170 °C in less than ~ 5 min under N_2 under a ~ 40 V/ μm applied electric field and held at 170 °C under the field, and scattering profiles were obtained every 5 min. Early stages of the development of order and orientation were examined as the copolymer was heated from a poorly ordered state into the ordered state under an applied external electric field (~ 40 V/ μm). Real time small-angle neutron scattering studies were performed on dPS-*b*-PMMA films on silicon substrates with the native oxide layer. Films having thicknesses of ~ 110 nm, ~ 700 nm, and ~ 3 μm were investigated.

For TEM, the copolymer films were heated to 170 °C under N_2 with a ~ 40 V/ μm applied electric field for a predetermined time and then quenched to room temperature before removing the field. The films for TEM were prepared on a substrate modified with random copolymer of styrene and methyl methacrylate having a 0.9 styrene fraction. A thin layer of carbon (10–20 nm) was coated onto the surface before the film was embedded in epoxy and cured at 60 °C for 12 h. The film was removed from the substrate by dipping into liquid N_2 , microtomed at room temperature with a diamond knife, and transferred to a copper grid. The thin sections were exposed to ruthenium tetroxide vapor for 30–35 min to enhance the

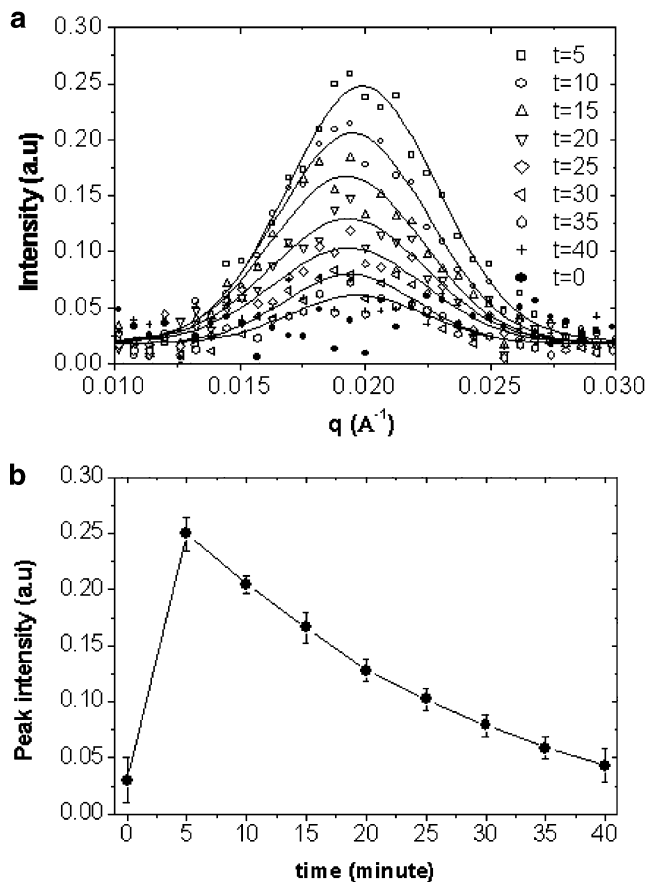


Figure 1. (a) Evolution of the SANS angular average intensity of the thin PS-*b*-PMMA film (~ 110 nm) annealing under ~ 40 V/ μm electric field. Solid line is the Gaussian fit of the data. (b) Evolution of the peak intensity with annealing time under electric field for the thin films.

contrast. Electron microscopy experiments were performed on a JEOL 100CX TEM at the accelerating voltage of 100 kV.

Results and Discussion

Figure 1a shows the evolution of the azimuthally averaged SANS intensity of a ~ 110 nm thick film at 170 °C under ~ 40 V/ μm electric field. At $t = 0$, i.e. immediately after spin-coating, a broad, weak peak is seen, indicating that the copolymer is poorly ordered. Upon heating to 170 °C a sharp reflection is seen in the SANS at $q^* = 0.02$ \AA^{-1} ($q = (4\pi/\lambda) \sin \theta$, where λ is the neutron wavelength, and 2θ is the scattering angle), corresponding to a period of ~ 31 nm. The peak intensity increased initially, reached a maximum, and then decreased with continued annealing. Shown in Figure 1b is the peak intensity as a function of time. The peak intensity at q^* is approximately proportional to the number of microdomains oriented along the applied electric field direction, i.e., normal to the surface. Thus, there is a rapid orientation of the lamellar microdomains normal to the surface. However, with time, the microdomains reorient parallel to the surface due to the preferential interactions of the PMMA with the oxide substrate. The evolution of the peak intensity reflects the competition between the applied electric field and interfacial interactions. For the 110 nm films, approximately four periods in thickness, interfacial interactions are seen to dominate as expected from calculations performed by Pereira and Williams¹⁴ and Tsori and Andelman.¹⁵

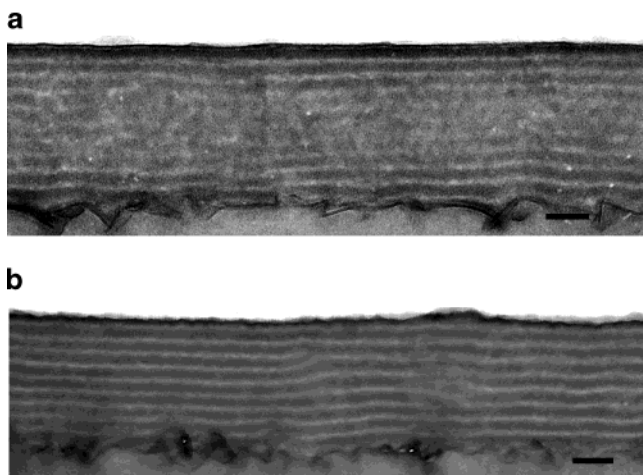


Figure 2. Cross-sectional TEM image of a ~ 300 nm PS-*b*-PMMA film annealed under ~ 40 V/ μm electric field for (a) 3 h and (b) 6 h. Scale bar: 100 nm.

Parts a and b of Figure 2 show the cross-sectional TEM images of ~ 300 nm thick dPS-*b*-PMMA films annealed under an electric field for 3 and 6 h, respectively, on a silicon substrate that has been modified with a random copolymer of styrene and methyl methacrylate having a styrene fraction of 0.9. After 3 h, the lamellar microdomains aligned parallel to both electrode interfaces due to the preferential wetting of the PS blocks. In the center of the film, however, the microdomains have mixed orientations with very small grain sizes. After 6 h, the lamellar microdomains are oriented parallel to the substrate interfaces throughout the film, even with the applied electric field normal to the interface. Annealing the film for 16 h did not change the microdomain orientation. Results from the TEM studies also indicate that the applied electric field is not sufficiently high to overcome the interfacial interactions, and the lamellar microdomains orient parallel to the surface.

Previous studies have shown that interfacial interactions have a limited range over which orientation propagates into the film. The range depends on the strength of interfacial interactions. The stronger the interactions, the greater is the distance that the orientation propagates into the film.²³ Beyond this range, however, fluctuations cannot be suppressed by the interface and different orientations appear. The coherence of the orientation across the films is lost after $\sim 5L_0$ for the substrate modified using 90/10 random copolymer of styrene and methyl methacrylate. A second set of in-situ SANS experiments was performed to follow the alignment of a dPS-*b*-PMMA thick film (~ 700 nm). Figure 3a shows the time evolution of the circularly averaged SANS from a ~ 700 nm film on the Si substrate with native oxide layer. At $t = 0$, i.e., after spin-coating, a broad, weak maximum is seen, indicating the copolymer is poorly ordered. Once heated above the glass transition temperature, the polymer chains become mobile and microphase separate under the influence of the applied electric field. The peak is seen to intensify rapidly (within the first 5 min) with a maximum at $q^* = 0.021 \text{ \AA}^{-1}$ and full width at half-maximum (FWHM) of 0.0074 \AA^{-1} . Further annealing causes the peak to intensify, shift to a smaller $q^* = 0.02 \text{ \AA}^{-1}$, and narrow with a FWHM of 0.0055 \AA^{-1} at $t = 25$ min. As shown in Figure 3b, the peak intensity initially increases rapidly, indicating that the number of the microdomains aligned

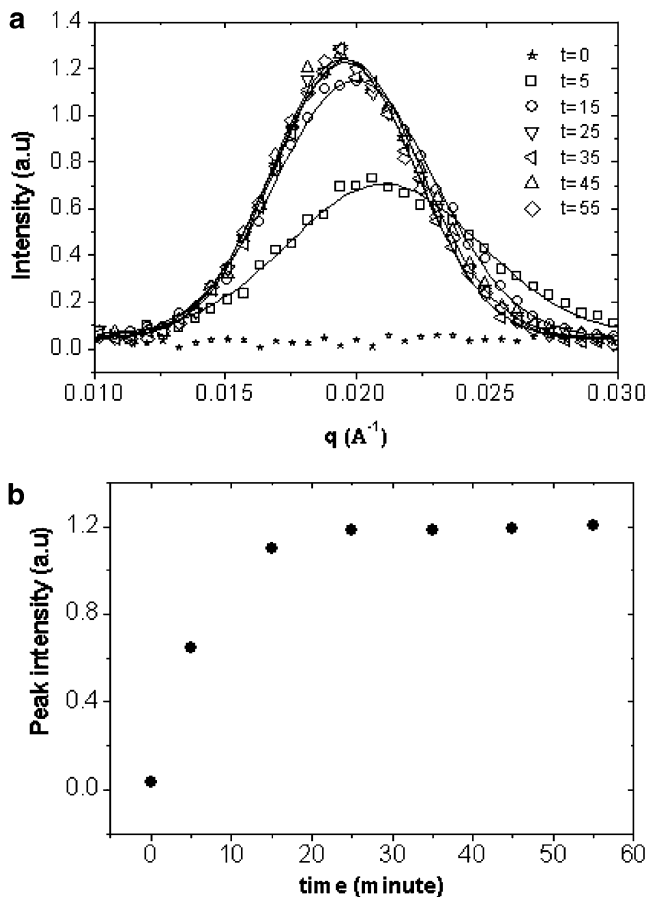


Figure 3. (a) Evolution of the SANS angular average intensity of the thick PS-*b*-PMMA film (~ 700 nm) annealing under ~ 40 V/ μm electric field. Solid line is the Gaussian fit of the data. (b) Evolution of the peak intensity with annealing time under electric field.

along the electric field direction has rapidly increased. Subsequently, the intensity increases only slowly. In comparison to thin films where the interfacial interactions dominate, in thicker films the applied electric field is more effective in orienting the microdomains.

Shown in parts a and b of Figure 4 are cross-sectional TEM images of a ~ 700 nm thick PS-*b*-PMMA film on a silicon substrate (modified with 90/10 random copolymer) that had been annealed under electric field for 6 and 16 h, respectively. Mixed orientations were observed and an orientation of the lamellar microdomains in the direction of the applied field is found in the middle of the films. This results from a kinetic trapping as discussed earlier.²² After annealing for 6 h, the lamellar microdomains near the electrode interfaces are aligned parallel to the interfaces, due to the preferential wetting of PS blocks with the electrodes. However, in the center of the film, the lamellar microdomains formed small anisotropic grains. Within these small grains, the microdomains are, on average, oriented in the direction of the applied electric field. After 16 h, the orientation of the microdomains by both electrode interfaces and the applied electric field is evident, as shown in Figure 4b. Consistent with previous studies, the parallel orientation extends $\sim 5L_0$ from both interfaces into the film before any orientation due to the applied field is evident.²²

Figure 5a shows the evolution of the circularly averaged SANS intensity for a $\sim 3 \mu\text{m}$ film. After spin-coating, $t = 0$, a diffuse, weak peak is seen at $q \approx 0.02$

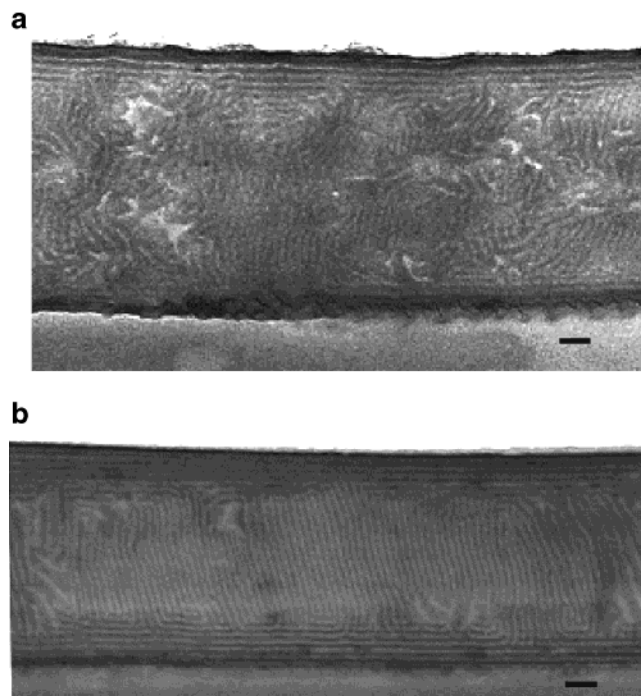


Figure 4. Cross-sectional TEM image of a ~ 700 nm PS-*b*-PMMA film annealed under ~ 40 V/ μm electric field for (a) 6 h and (b) 16 h. Scale bar: 100 nm.

\AA^{-1} with a FWHM of 0.005 \AA^{-1} . This is similar to the results observed for the thinner films. With increasing time, the peak intensifies, narrows, and shifts to a slightly smaller q . From the peak intensity in Figure 5b, the orientation is seen to continue steadily, even after annealing under the applied field for 6 h.

Shown in Figure 6a is the cross-sectional TEM images of a film annealed under electric field for 3 h. The microdomains adjacent to the interfaces are aligned parallel to the surface due to the preferential wetting of PS blocks. Though SANS shows very strong scattering for the samples subjected to the same treatment, only very small grains were seen in the center of the film, and the orientation of microdomains is not immediately clear. Figure 6b is the cross-sectional TEM images of a film annealed under electric field for 6 h. The lamellar microdomains are easily seen and the grain size has increased. The orientation of the microdomains is along the electric field direction, though there are still microdomains with no preferred orientation. In this image, there are several distinct features (labeled A, B, C) that provide insight into the alignment process. In all the A type regions, there are ellipsoidal grains with their long axis parallel to the surface. The lamellar microdomains within these grains are aligned parallel to the electric field direction. In regions marked B, the lamellar microdomains have random orientation. Here grains are very small with many defects in the stacking of the lamellae. Some of the lamellar microdomains are disrupted and are melding with nearby microdomains. In regions marked C, the disruption and melding process are clearly manifest. Fluctuations with a period similar to that of the equilibrium lamellar period are evident, in contrast to the classical Helfrich–Hurault undulations calculated for smectic and cholesteric liquid crystals. Both conformal and nonconformal fluctuations in adjacent lamellae can be seen, with nonconformal fluctuations prevalent in the lamellae adjacent to the substrate, in agreement with Tsori and

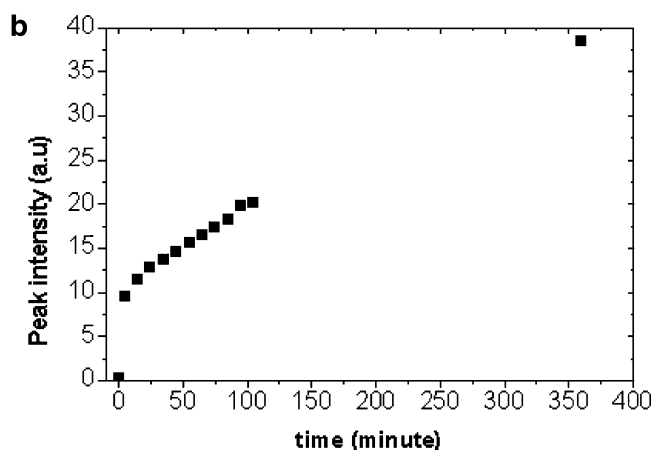
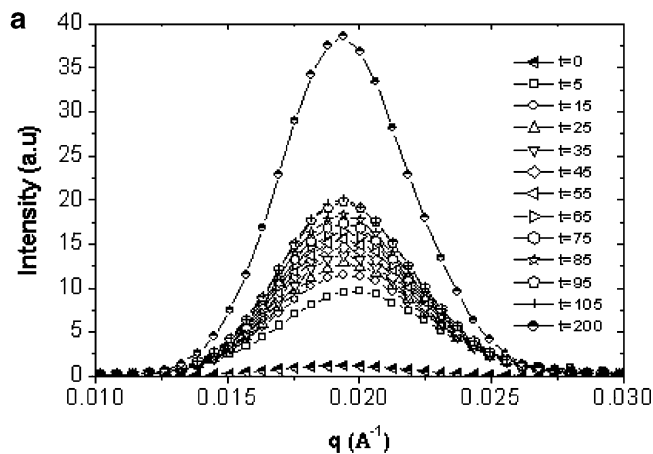


Figure 5. Evolution of the SANS angular average intensity of the thicker PS-*b*-PMMA film ($\sim 3 \mu\text{m}$) annealing under ~ 40 V/ μm electric field. Solid line is the Gaussian fit of the data. (b) Evolution of the peak intensity with annealing time under electric field.

Andelman¹⁵ and Fukuda and Onuki.¹⁸ There are striking similarities between the TEM images shown here and the images shown in the simulations of Zvelindovsky.²⁰ The movement and coalescence of the defects, i.e., the local disruption and re-formation of lamellae, appears to be the dominant pathway in achieving alignment.

A cross-sectional TEM image of a film annealed under electric field for 16 h is shown in Figure 6c. Throughout the image, the lamellar microdomains are aligned parallel to the field direction. The number of defects is substantially reduced, though slight misalignment of adjacent grains still exists. Removal of this misalignment, however, requires extended annealing, since the driving force to perfectly align the domains parallel to the applied field is small.

Conclusion

Electric field alignment of symmetric diblock copolymer thin films was studied using in-situ small-angle neutron scattering and transmission electron microscopy. The early stage of the alignment process was found to be a competition between the applied electric field strength and the interfacial interactions. For thin films, the surface-induced orientation dominates and the lamellar microdomains remain parallel to the substrate surface, independent of the strength of the applied electric field. With increasing film thickness, surface

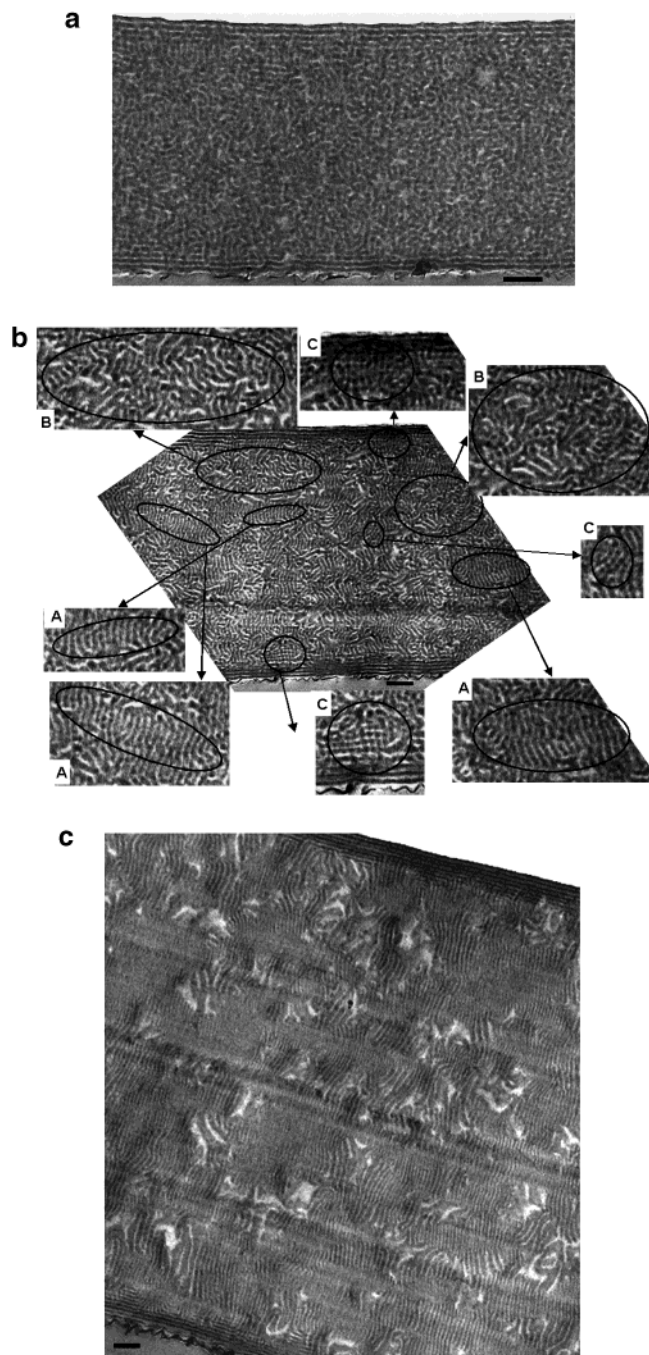


Figure 6. Cross-sectional TEM image of PS-*b*-PMMA films annealed under ~ 40 V/ μm electric field for (a) 3 h, (b) 6 h, and (c) 16 h. Scale bar: 200 nm.

effects dissipate with distance from the surface, and in the interior of the film, the lamellar microdomains were oriented normal to the surface, i.e., parallel to the direction of the applied electric field. The migration and coalescence of the defects were found to be the dominant

pathways to align the lamellar microdomains in the direction of the applied field.

Acknowledgment. This work was supported by the Army Research Laboratory, Polymer Center of Excellence at the University of Massachusetts, Amherst, the Department of Energy, Office of Energy Sciences (DEFG02-96ER45), and the National Science Foundation-supported Material Research Science and Engineering Center (MRSEC) at University of Massachusetts, Amherst (DMR-9400488). We acknowledge the support of the National Institute of Standards and Technology, U.S. Department of Commerce, in providing the neutron research facilities used in this work. This work utilized facilities supported in part by the National Science Foundation under Agreement DMR-9986442 and the Keck Foundation. We thank Dr. Hammond, Dr. S. Kline, and Dr. D. Ho at NIST for assistance with the neutron scattering measurements.

References and Notes

- (1) Bates, F. S.; Fredrickson, G. H. *Annu. Rev. Phys. Chem.* **1990**, *41*, 5252.
- (2) Keller, A.; Pedemonte, E.; Willmouth, F. M. *Nature (London)* **1970**, *225*, 538.
- (3) Albalak, R. J.; Thomas, E. L. *J. Polym. Sci., Polym. Phys.* **1993**, *31*, 37.
- (4) Albalak, R. J.; Thomas, E. L. *J. Polym. Sci., Polym. Phys.* **1994**, *32*, 341.
- (5) Thurn-Albrecht, T.; DeRouchey, J.; Russell, T. P.; Jaeger, H. M. *Macromolecules* **2000**, *33*, 3250.
- (6) Thurn-Albrecht, T.; Schotter, J.; Kastle, C. A.; Emley, N.; Shibauchi, T.; Krusin-Elbaum, L.; Guarini, K.; Black, C. T.; Tuominen, M. T.; Russell, T. P. *Science* **2000**, *290*, 2126–2129.
- (7) Huang, E.; Rockford, L.; Russell, T. P.; Hawker, C. J. *Nature (London)* **1998**, *395*, 757.
- (8) Amundson, K.; Helfand, E.; Davis, D. D.; Quan, X.; Patel, S. S.; Smith, S. D. *Macromolecules* **1991**, *24*, 6546.
- (9) Amundson, K.; Helfand, E.; Quan, X.; Smith, S. D. *Macromolecules* **1993**, *26*, 2698.
- (10) Amundson, K.; Helfand, E.; Quan, X. N.; Hudson, S. D.; Smith, S. D. *Macromolecules* **1994**, *27*, 6559.
- (11) Hasegawa, H.; Hashimoto, T. *Macromolecules* **1985**, *18*, 589.
- (12) Anastasiadis, S. H.; Russell, T. P.; Satija, S. K.; Majkrzak, C. F. *J. Chem. Phys.* **1990**, *92*, 5677.
- (13) Anastasiadis, S. H.; Russell, T. P.; Satija, S. K.; Majkrzak, C. F. *Phys. Rev. Lett.* **1989**, *62*, 1852.
- (14) Pereira, G. G.; Williams, D. R. M. *Macromolecules* **1999**, *32*, 8115.
- (15) Tsori, Y.; Andelman, D. *Macromolecules* **2002**, *35*, 5161–5170.
- (16) Boker, A.; Knoll, A.; Elbs, H.; Abetz, V.; Muller, A. H. E.; Krausch, G. *Macromolecules* **2002**, *35*, 1319.
- (17) Boker, A.; Elbs, H.; Hansel, H.; Knoll, A.; Ludwigs, S.; Zettl, H.; Urban, V.; Abetz, V.; Muller, A. H. E.; Krausch, G. *Phys. Rev. Lett.* **2002**, *89*, 135502.
- (18) Fukuda, J.; Onuki, A. *J. Phys. II* **1995**, *5*, 1107–1113.
- (19) Zvelindovsky, A. V.; Sevink, G. J. A. *Phys. Rev. Lett.* **2003**, *90*, 49601.
- (20) Kyrlyuk, A. V.; Zvelindovsky, A. V.; Sevink, G. J. A.; Fraaije, J. G. E. M. *Macromolecules* **2002**, *35*, 1473.
- (21) DeRouchey, J.; Russell, T. P. Unpublished results, 2003.
- (22) Xu, T.; Hawker, C. J.; Russell, T. P. *Macromolecules* **2003**, *36*, 6178.
- (23) Xu, T.; Hawker, C. J.; Russell, T. P. Manuscript in preparation.

MA035805G